Published in final edited form as:
Clin Cancer Res. 2012 March 1; 18(5): 1291–1302. doi:10.1158/1078-0432.CCR-11-0950.

Polymeric Nanoparticle Encapsulated Hedgehog Pathway Inhibitor HPI-1 ("NanoHHI") Inhibits Systemic Metastases in an Orthotopic Model of Human Hepatocellular Carcinoma

Yang Xu[1,2,*], **Venugopal Chenna**[2,*], **Chaoxin Hu**[2], **Hai-Xiang Sun**[1,2,4], **Mehtab Khan**[2], **Haibo Bai**[2], **Xin-Rong Yang**[1], **Qin-Feng Zhu**[2,4], **Yun-Fan Sun**[1], **Anirban Maitra**[2,3], **Jia Fan**[1,4], and **Robert A. Anders**[2]

[1]Liver Cancer Institute, Zhong Shan Hospital and Shanghai Medical School, Fudan University, Key Laboratory for Carcinogenesis & Cancer Invasion, The Chinese Ministry of Education, Shanghai, PR China [2]The Sol Goldman Pancreatic Cancer Research Center, Department of Pathology, Johns Hopkins University School of Medicine, Baltimore, Maryland [3]The Sol Goldman Pancreatic Cancer Research Center, Department of Oncology, Johns Hopkins University School of Medicine, Baltimore, Maryland [4]Institute of Biomedical Sciences, Fudan University, Shanghai, PR China

Abstract

Purpose—To illustrate the prognostic significance of hedgehog (Hh) signaling in hepatocellular carcinoma (HCC) patients, and to evaluate the efficacy of a novel nanoparticle-encapsulated inhibitor of the Hh transcription factor, Gli-1 ("NanoHHI") using *in vitro* and *in vivo* models of human HCC.

Experimental Design—Patched1 (Ptch1) expression was detected in tumor tissue microarrays of 396 HCC patients who underwent curative surgical resection during 2/2000 to 12/2002. Prognostic significance was assessed using Kaplan-Meier survival estimates and log-rank tests. The effects of NanoHHI alone and in combination with sorafenib were investigated on HCC cell lines. Primary HCC tumor growth and metastasis were examined *in vivo* using subcutaneous and orthotopic HCC xenografts in nude mice.

Results—Elevated expression of Ptch1 in HCC tissues was significantly related to disease recurrence, as well as a shorter time to recurrence in HCC patients. *In vitro*, NanoHHI significantly inhibited the proliferation and invasion of HCC cell lines. NanoHHI potently suppressed *in vivo* tumor growth of HCC xenografts in both subcutaneous and orthotopic milieus, and in contrast to sorafenib, resulted in significant attenuation of systemic metastases in the orthotopic setting. Further, NanoHHI significantly decreased the population of CD133-expressing HCC cells, which have been implicated in tumor initiation and metastases.

Conclusion—Downstream Hh signaling has prognostic significance in HCC patients as it predicts early recurrence. Gli inhibition through NanoHHI has profound tumor growth inhibition and anti-metastatic effects in HCC models, which may provide a new strategy in the treatment of HCC patients and prevention post-operative recurrence.

Correspondence to: Robert A. Anders, M.D., Ph.D., Department of Pathology, Division of Gastrointestinal and Liver Pathology, Room 346, CRB-II, Johns Hopkins University School of Medicine, 1550 Orleans St, Baltimore, MD 21231, USA. Tel: 410-955-3511, Fax: 410-614-0671. rander54@jhmi.edu or Jia Fan, M.D., Ph.D., Liver Cancer Institute, Fudan University, 136 Yi Xue Yuan Road, Shanghai 200032, P. R. China. Tel. & Fax: +86-21-64037181. jiafan99@yahoo.com.
*YX and VC contributed equally to this manuscript.

Keywords

Hepatocellular carcinoma; Hedgehog; smoothened; Gli1; HPI-1; polymeric nanoparticle; NanoHHI

Introduction

Hepatocellular carcinoma (HCC) is the third leading cause of cancer death world-wide, and the age-adjusted incidence rates have doubled over the past two decades (1, 2). Despite the advancement of therapeutic modalities including surgery and chemotherapy, the overall survival (OS) of patients with HCC remains unsatisfactory because of the high rate of recurrence and metastasis (3, 4). Sorafenib, a novel multikinase inhibitor, is the only targeting molecule which has recently been approved by Food and Drug Administration for the treatment of unresectable HCC. Nevertheless, sorafenib only showed limited survival benefits in the late stage HCC patients, and has no strong efficacy on tumor metastasis, which is the most common cause of death from HCC (5, 6). Hence, there is a pressing need for novel targeted pathway and alternative therapeutic modalities for treating HCC.

The Hedgehog (Hh) pathway is a major tissue growth regulator. The pathway is activated by the binding of mammalian Hh ligands (Sonic Hh, Indian Hh and Desert Hh) to Patched (Ptch1) which relieves its inhibition on Smoothened (Smo), culminating in the nuclear localization of DNA-binding Gli transcription factors. These transcription factors lead to production of Hh target genes, such as *Ptch1* and *Gli1*, which also serve as convenient readouts of pathway activation. Together these components generally function to control tissue development of many tissue types. (7–9). For example, in the fetus this signaling pathway functions early in the endoderm to establish hepatic progenitor cells (10). However, Hh signaling appears to have a far more significant role in maintaining hepatic progenitors in the adult liver (11, 12) (13). The Hh pathway is activated during liver regeneration (13) and in response to chronic liver injury (11, 12, 14, 15).

Inappropriate activation of Hh pathway has been implicated in several gastrointestinal tumor types (16). Several studies have demonstrated aberrant Hh signaling in human HCC tissues and cell lines. Hh signaling appears to be particularly active in the setting of chronic liver disease and might partially account for the common occurrence of HCC in the setting of chronic liver disease and cirrhosis (17, 18). Blockade of Hh signaling results in decreased proliferation and migration, and an increase in apoptosis of human HCC cell lines (19–26). Other groups have implicated Hh transcriptional targets as critical to tumor progression and metastasis (21, 23).

Of the multiple small molecule Hh inhibitors currently undergoing evaluation in clinical trials, all are Smo antagonists (27). However, there are two potential shortcoming for targeting Smo in human cancers. First, is the recently described ability of tumors to secondarily acquire *Smo* mutations that can abrogate the ability of antagonists to bind to the heptahelical bundle of Smo protein (28–31). Secondly, Smo independent pathways leading to Gli activation have been demonstrated recently by Hanahan and colleagues. For these reasons, and evidence showing that RNA-mediated interference of *Gli1* causes apoptosis in human HCC cell lines but not in normal hepatocytes (20), we evaluated whether a direct inhibitor of Gli which might provide improved therapeutic advantage in HCC.

Recently four Hh pathway inhibitors (HPIs 1–4) have been identified that block Hh signaling downstream of Smo (32). In particular, HPI-1 is a potent antagonist of Gli proteins (Gli-1 and 2) and also blocks Hh signaling in the setting of exogenous Gli expression.

However it might be difficult to translate these *in vitro* findings to *in vivo* studies since this inhibitor has poor systemic bioavalibility. Its lipophilic nature and poor aqueous solubility make it difficult to deliver *in vivo*. We developed and characterized(33) a novel polymeric nanoparticle encapsulating HPI-1 (NanoHHI).

In this study we first established the clinical significance of Ptch1 expression in HCC, as a marker of downstream Hh activity. We show Ptch1 expression in patients undergoing curative HCC resection correlated with early recurrence and was a poor prognostic feature. Further, we show that NanoHHI is effective at inhibiting the proliferation and motility of two human HCC cell lines *in vitro*, and significantly inhibits subcutaneous tumor growth at least as effectively as the current standard-of-care chemotherapeutic agent, sorafenib. Notably, however, NanoHHI is remarkably more effectively than sorafenib at inhibiting metastasis in a lethal orthotopic model of human HCC. The ability to potently suppress systemic metastasis is likely attributed to the ability of NanoHHI to significantly down regulate CD133-expressing cells, which are implicated as tumor initiating cells in HCC. These studies provide early evidence of a nanoparticle encapsulated agent that might be useful for chemotherapy in patients at high risk of HCC recurrence after curative surgical resection.

Materials and Methods

Patients and Specimens

Tumor specimens used in TMAs were obtained from 396 HCC patients who underwent surgical resection at the Liver Cancer Institute, Zhong Shan Hospital, Fudan University from Feb 1st, 2000 to Dec 1st, 2002. Tumor specimens were taken from viable areas of the tumors; necrotic tissues were avoided. The inclusion criteria of all the patients in this study were (1) confirmed histopathological diagnosis of HCC based on the WHO criteria (34); (2) without any prior therapy; (3) with an “intent-to-cure” surgical resection, which is defined as the complete resection of all tumor nodules and the margins being free of cancer by histological examination(35); (4) with suitable formalin-fixed, paraffin-embedded tissues; and (5) patients with demographic and clinicopathological follow-up data. Tumor differentiation was defined according to the Edmondson grading system (36). Liver function was assessed by the Child-Pugh classification. Tumor staging was defined according to the sixth edition of TNM classification of UICC. The clinicopathological characteristics of all the patients were summarized in Table 1. Ethical approval for human subjects was obtained from the research ethics committee of Zhong Shan Hospital and the Johns Hopkins University Institutional Review Board.

Follow-up and Tumor Recurrences

Patients were followed up every 2 months during the first postoperative year and at least every 3–4 months afterward. Follow-up was obtained until March 30, 2010. All patients were prospectively monitored by serum alpha-fetoprotein (AFP), abdominal ultrasonography and chest x-ray every 1–6 months in the postoperative period. A computed-tomography (CT) scan of the abdomen was performed every 6 months. Bone scan or magnetic resonance imaging (MRI) was done if localized bone pain was reported. If recurrence was suspected, CT scan or MRI was performed immediately. Most patients died from recurrence or metastasis, or complicated liver cirrhosis. Patients with confirmed recurrence received further treatment, which followed the same protocol based on the size, site, number of tumor nodules and liver function. Briefly, if the recurrent tumor was localized, a second liver resection, radiofrequency ablation (RFA), or percutaneous ethanol injection (PEI) was performed; if the recurrent tumor was multiple or diffuse, then transcatheter arterial chemoembolization (TACE) was the choice. External radiotherapy was

given if lymph node or bone metastasis was found. Otherwise, symptomatic treatment was provided. Overall survival (OS) was defined as the interval between surgery and death or the last observation taken. The data were censored at the last follow-up for living patients. Time to recurrence (TTR) was measured from the date of resection until the detection of recurrent tumor and data were censored for patients without signs of recurrence.

Tissue Microarray and Immunohistochemistry

TMA was constructed as previously described (37). Briefly, all the HCC and peritumoral liver tissues were reviewed by two histopathologists, and representative areas free from necrotic and hemorrhagic materials were pre-marked in the paraffin blocks. Two core biopsies of 1mm in diameter were taken from the donor blocks and transferred to the recipient paraffin block at defined array positions. Two HCC and 2 respective peritumoral liver TMA blocks were constructed. Consecutive sections of 4-μm thickness were taken on 3-aminopropyltriethoxysilane (APES)-coated slides (Shanghai Biochip Co., Ltd., Shanghai, P.R.China). The rabbit polyclonal antibody for Ptch1 was purchased from Santa Cruz Biotechnology, Santa Cruz, CA (No. sc-6149, diluted 1:100). Immunohistochemistry was carried out using a two-step protocol (Novolink Polymer Detection System, Novocastra, Newcastle, UK) as previously described (37, 38). Briefly, after microwave antigen retrieval, tissues were incubated with primary antibodies for 60 min at room temperature or overnight at 4°C. Following 30 min incubation with secondary antibody (A0545, sigma), the sections were developed in DAB solution under microscopic observation and counterstained with hematoxylin. Negative control slides with the primary antibodies omitted were included in all assays.

Evaluation of Immunohistochemical Variables

Immunohistochemical staining was assessed by two independent pathologists without knowledge of patient characteristics. Staining score of Ptch1 was calculated according to the percentage of positive cells (cytoplasm) from 0 to 100, and the samples in the cohort were classified as negative when the scores ranged from 0 to 25 and positive when they fell between 26 and 100 based upon ROC curve (Supplemental Figure S1). All of the cases with different scorings were discussed at a multi-headed microscope until consensus was reached. The duplicate of spots for each tumor showed relative homogeneity for stained cell percent and intensity. The higher score was considered as a final score in case of a difference between duplicate tissue cores.

Drugs Formulations

NanoHHI was engineered as described(33). Sorafenib was purchased from Bayer Pharmaceutical Corporation, and dissolved in sterile DMSO and stored frozen under light-protected conditions at −20 °C.

Cell culture

Huh7, HepG2, and MHCC97L (97L) human HCC cell lines were used in these studies. Huh7 and hepG2 were purchased from America Type Culture Collection. 97H and 97L were provided by Dr. Xin-Wei Wang from U.S. National Cancer Institute with the permission of Prof. Zhao-You Tang of Liver Cancer Institute, Fudan University, China. All the cell lines were routinely maintained were maintained at 37°C and 5% CO2 in DMEM supplemented with 10% fetal bovine serum (FBS) and 1% penicillin/streptomycin.

In vitro Growth and Matrigel Invasion Assay

Cell proliferation was assessed using the MTT assay. Cells were seeded at a density of 2000 cells per well and allowed to grow overnight. Huh7 and MHCC97-L cells were treated with

NanoHHI (40μM), sorafenib (10μM) or NanoHHI (40μM)+sorafenib (10μM). Cell viability was measured after 48 h. Huh7 and MHCC97-L cells were seeded onto a Matrigel-coated filter (No.3458, Corning) containing NanoHHI (40μM), sorafenib (10μM) or NanoHHI (40μM)+sorafenib (10μM) for the cell invasion assay and incubated for 8 h at 37°C. The cells that actively migrated to the lower surface of the filters were stained and quantified. All assays were performed in triplicate.

In vivo preclinical studies on NanoHHI efficacy

Male athymic BALB/c nu/nu mice, 4 – 6 wk old, were purchased from Jackson Laboratory. All studies on mice were conducted in accordance with the National Institutes of Health "Guide for the Care and Use of Laboratory Animals". The study protocol was approved by Medical Experimental Animal Care Committee of Johns Hopkins University. Subcutaneous and orthotopic HCC models were established as described before (25). Briefly, approximately 5×10^6 Huh7 cells in 0.2 ml culture medium were injected subcutaneously into the right flank of athymic mice, which were then observed daily for signs of tumor development. Once the subcutaneous tumor reached 1 cm in diameter, it was removed and freshly minced into pieces about $2mm^3$, which were implanted into the liver of athymic mice, using the method as described previously (25). The subcutaneous and orthotopic models were administered drugs beginning at day 7 following tumor cell injection or tumor implantation. Twenty subcutaneous and 20 orthotopic tumor mice were randomly assigned to four experimental groups. The four experimental groups were as follows: untreated control group, NanoHHI (30mg/kg, i.p, twice a day for 4 weeks), sorafenib (20mg/kg, orally take by gavage in 1% DMSO, twice a day for 4 weeks) treatment group, and NanoHHI combined sorafenib treatment group (administered by using the same schedule for each drug as described for the single treatment). All control mice received an equal volume of carrier solution by gavage and injection, respectively. The mice were sacrificed 4 weeks after treatment. At necropsy, tumor volume was measured for largest (a) and smallest (b) diameters, and the tumor volume was calculated as $V = a\times b^2/2$. Tumors were either homogenized for Western blot analysis and qRT-PCR, or fixed in paraformaldehyde for 24 h, and paraffin sections were used for immunohistochemical staining. Metastatic implants in abdominal and thoracic organs and surfaces were determined at the time of necropsy by serial sectioning of organs coupled with gross and histologic inspection. Paraffin blocks of 10% buffered formalin-fixed samples of lung were prepared and serial sections were cut at 4μm and stained with H&E to determine the presence of lung metastases.

QRT-PCR, Western blot, and Flow cytometry

Total RNA was prepared using Trizol (Invitrogen), and then cDNA was synthesized using the Superscript First-Strand Synthesis system (Invitrogen). Quantitative real time qRT-PCR amplification for human Gli-1 (hGli1), Gli-2 (hGli2), and murine Gli1 (mGli1), Gli-2 (mGli2) was performed with TaqMan Fast Universal PCR Master Mix with (Applied Biosystem Carlsbad, CA). The qRT-PCR was performed with an Applied Biosystem Step One Plus system using *beta-actin* (assay ID Mm01205647, reference sequence ID NM_001101.2) as housekeeping control. The assay ID for *mGli1* is 00494645_m1 and the reference sequence is NM_010296.2. Relative mRNA levels were calculated based on the $2^{-\Delta\Delta CT}$ method. Anti-human CD133-PE antibody (No. 130-080-801, MACS) was used for CD133 immunofluorescent detection by flow cytometry. Isotope-matched mouse immunoglobulin (No. 130-092-212, MACS) was incorporated as controls. Cells were incubated in phosphate-buffered saline (PBS) containing 2% fetal bovine serum (FBS) and 0.1% sodium azide with fluorescence-conjugated primary antibody. Samples were analyzed using a FACSCalibur flow cytometer and CellQuest software (BD Biosciences, San Jose, CA).

Statistical Analysis

Statistical analyses were performed by SPSS 15.0 for windows (SPSS, Chicago, IL). Cumulative survival time was calculated by the Kaplan-Meier method and analyzed by the log-rank test. Univariate and multivariate analyses were based on the Cox proportional hazards regression model. The chi-square test, Fisher's exact probability and student's t-test were used for comparison between groups. $P<0.05$ was considered statistically significant.

Results

Expression of Ptch1 and Relevance to Prognostic Factors

There are reports of Hh signaling components expressed in human HCC tissues, however, these results have not been linked to clinical outcome (21, 39). We examined Ptch1 expression, as a downstream marker of Hh activation, using immunohistochemical staining of a tissue microarray constructed from 396 patients who had undergone HCC resection with curative intent. The clinical and pathologic characteristics of this patient cohort revealed 207 (52%) patients were over 50 years of age, 346 (87.4%) were men with 324 (81.8%) infected with chronic hepatitis B (Table 1). Ptch1 expression was detected in 101 (25.5%) HCC tumor samples, whereas only 33 (8.3%) of the non-tumor tissue yielded positive Ptch1 labeling (Table 1). The expression of Ptch1 was significantly elevated in tumor tissue samples compared with the non-tumor counterparts ($P<0.01$). Staining was relatively homogenous within a neoplasm, excluding necrotic, hemorrhagic and fibrotic regions. Compared to control staining, Ptch1 was detected predominantly in the cytoplasm of tumor cells, and was also present to a lesser extent at the cell membrane (Figure 1A-D). Ptch1 expression in tumor tissue correlated with patient age of presentation, tumor encapsulation and recurrence (Table 2). For the whole study population, the 5-year overall survival (OS) and time to recurrence (TTR) rates were 53.4% and 46.3% respectively. On univariate analysis, significant poor predictors of OS included serum HBsAg; Child-Pugh score; serum GGT and AFP; tumor encapsulation, size and number; vascular invasion; TNM and BCLC stage (Table 3). Significant factors associated with TTR were the number of tumors, vascular invasion, advanced TNM stage and Ptch1 expression. On multivariate analysis, AFP and tumor size were independent factors associated with OS. Ptch1 expression was an independent predictive factor of TTR (Table 4). Patients with Ptch1 expressing tumors had significantly reduced mean time to relapse compared to those without Ptch1 expression (5y-TTR: 43.7% *vs.* 54.3%, $P=0.029$, Figures 1E and 1F). The significant prognostic role of Ptch1 was also apparent in late stage HCC patients (TNM II-III, $P=0.027$), and the patients with well differentiated tumors (Edmondson grade I-II, $p=0.021$, Figure 1G & 1H). This series of data shows downstream Hh signaling appears to correlate with HCC recurrence.

NanoHHI inhibits HCC cell proliferation and invasion in vitro

We wanted to determine if suppressing downstream Hh activity with a potent Gli inhibitor could inhibit the *in vitro* growth of HCC cell lines(33). We found NanoHHI significantly ($P<0.029$) suppressed Huh7 cell growth compared to vehicle control and to a comparable degree as sorafenib (Figure 2A). In another human HCC cell line, MHCC-97L, sorafenib significantly suppressed *in vitro* growth, while, NanoHHI showed some growth suppression, but this was not statistically different than control ($P>0.05$) (Figure 2A). Since downstream Hh activity is associated with HCC invasion (21, 23) we next measured the ability of NanoHHI to inhibit invasion. We found NanoHHI significantly suppressed the ability of both Huh7 and MHCC-97L cells to invade into Matrigel compared to vehicle treatment (Figure 2B & 2C). Similarly, sorafenib significantly inhibited HCC invasion *in vitro* in both cell lines, with a minor but not statistically significant additive effect when cells were treated with both NanoHHI and sorafenib (Figure 2B & 2C).

NanoHHI potently inhibits HCC growth and metastasis in vivo

One week after subcutaneous injection of the Huh7 cell line into athymic mice, they received treatment with vehicle, NanoHHI (NH 30 mg/kg twice daily i.p.), sorafenib (SO 20 mg/kg twice daily, p.o.), or both. After 4 weeks of treatments, tumor tissues were collected. No demonstrable adverse effects such as body weight loss were observed in any the groups. The weight of the subcutaneous xenografts in the mice in all three treatment groups were significantly decreased compared with those in vehicle group (Figure 3A, $P<0.05$). As expected, transcript analysis in the Huh7 cell line show NanoHHI treatment significantly suppresses human Gli1 and Gli2 (hGli1, hGli2) consistent with the well characterized Hh inhibitory role of the parental molecule (32) Sorafenib had little effect on hGli1 but did show a decrease in hGli2 expression (Figure 3C). The treated xenografts demonstrated significant reduction in hGli1 and hGli2 as well as murine Gli1 and Gli2 (mGli1, mGli2) levels (Figure 3D, E). Of note, there was no significant decrease in hGli1, hGli2 or mGli1, mGli2 expression in the sorafenib treated xenografts. In tumors receiving combination therapy there was significant suppression of hGli1 and mGli2

For orthotopic xenograft studies, a sterile $2mm^3$ piece of subcutaneous Huh7 tumor was implanted orthotopically into athymic nude male mice. After one week of implantation, treatment with NanoHHI (NH 30 mg/kg twice daily), sorafenib (SO 20 mg/kg), or both agents was initiated for a period of 4 weeks. At the end of the treatment, orthotopic liver xenografts were harvested. At the time of harvest, grossly evident peritoneal metastasis were recorded and liver, lung and lymph nodes were collected for histologic examination. A total of 16 tumor metastasis involving the liver, lung, peritoneum, mesentery, diaphragm and lymph nodes were found in all (5/5 mice) of the mice of control group, and 15 metastasis were found in (3/5 mice) in the sorafenib group (Figure 3B). Remarkably, only 2 metastases were found in 2 mice of NanoHHI group (Figure 3B). These were satellite, intrahepatic spread of tumors that were physically discontinuous from the initial tumor implant and not distant metastasis. Similarly, only 3 total metastatic lesions were found in the mice treated with both NanoHHI and sorafenib (Figure 3B). Taken as a whole, these data show that NanoHHI treatment potently suppresses HCC metastases.

NanoHHI decreases the population of CD133 positive HCC cells

To begin to understand how NanoHHI could suppress metastatic spread, we examined CD133 expression since it has been linked to Hh signaling and identifies a subpopulation of cancer initiating cells which could account for formation of metastasis(19). First we found NanoHHI treatment significantly downregulated CD133 mRNA in the orthotopic liver tumors harvested 4 weeks after the indicated treatments compared to control treatment *(P*<0.05 Figure 3F). Sorafenib and combination treatment also showed a decrease in CD133. Since CD133 expression is not unique to cancer initiating cells (19, 40, 41), we also looked at these treatments on Huh7 cells *in vitro*. We saw sorafenib treatment did not show a significant inhibition of CD133, while NanoHHI and combination treatment with both agents did significantly downregulate CD133 transcription (Figure 3G). This was also true after extended sorafenib treatment period at more than one dose (Supplemental Figure S2). Flow cytometry analysis showed that NanoHHI significantly decreased the population of CD133 positive cells compared with control (4.5% vs. 21.1%, $P<0.01$, Figure 3I). Again, sorafenib showed a trend to decreased CD133 surface expression but it was not statistically significant. (19, 40–42) As expected, sorafenib significantly decreased the expression of p-ERK *in vitro* and *in vivo* compared to control treatment as determined by Western blot (Figure 3H). Combination treatment of Huh7 cells with both NanoHHI and sorafenib showed a similar decrease as was seen with sorafenib alone. Collectively, these data support that inhibiting Hh with NanoHHI suppresses CD133 positive HCC tumor initiating cells, and leads to the observed reduction in systemic *in vivo* metastases.

Discussion

Survival for HCC remains dismal with surgical resection offering the best hope for cure. However, recurrent HCC occurs in a staggering 50 to 80% of patients with most occurring in the first 2 years (1, 3). It is not clear if early recurrence occurs due to residual microscopic foci of malignant cells undetectable at the time of surgery, dissemination during surgery or formation of de novo tumors(43). Regardless, there is significant need to target pathways responsible for HCC recurrence and develop therapies specifically aimed at preventing or delaying HCC recurrence and metastasis.

Activity of Hh signaling in the liver has been documented. Hh ligands are significantly expressed in diseased human liver tissue and cirrhosis (17, 18). This is particularly important since a majority of HCC occur in the setting of cirrhosis. Increased Hh activity has been shown in HCC (19–26). We found increased Ptch1 expression in HCC was a significant poor prognostic factor for patients undergoing curative resection. This was also true in patients with more advanced disease. Interestingly, at least two other studies have documented increased Hh activity and an association with invasion (21, 23). This data taken in the context of other publications provides rationale for suppressing Gli activity in treating HCC and particularly in preventing the vexing problem of post-surgical recurrence.

Current Hh signaling suppressive agents target at the level of Smo. However, this might not be the ideal target in hepatocellular carcinoma. Rare primary *Smo* mutations have also been reported in HCC, although the significance of these mutations to antagonist binding is unknown (26). TGF-beta is capable of Smo independent stimulation of Gli-1(44). TGFβ activity is particularly important in HCC since this pathway's activity correlates with poor clinical outcome (26, 31, 45). Second, malignancies develop secondary, non-oncogenic Smo mutations that make cells resistant to Smo antagonists (46–48). Mutation of Smo has been specifically reported in HCC (26). Targeting Ptch1 might not be ideal either since polymorphism in *Ptch1* have been linked to HCC differentiation and the functional significance of these polymorphisms is not clear (39). Finally, the downstream Hh target, *GLI1* is amplified in cancers but has not been specifically described in HCC (28, 29). For these reasons, we aimed to suppress the downstream Hh target Gli-1.

To suppress Gli activity we turned to HPI-1, a molecule Hyman and colleagues uncovered in a screen of small molecules aimed at suppressing Hh activity downstream of Smo(32). However, the native HPI-1 molecule is lipophilic and not water soluble which will likely translate into poor bioavailability. Therefore we used a polymeric nanoparticle encapsulated formulation (NanoHHI) which has been developed as a non-toxic, safe for *in vivo* studies Gli inhibitor(33).

We found NanoHHI significantly inhibited HCC proliferation and invasion to a similar degree as sorafenib *in vitro*. A striking difference was seen *in vivo*, with NanoHHI potently suppressing metastatic spread while sorafenib had practically no effect. A recent report addressed a similar question(49). Like Feng and Wang, we both show sorafenib decreases tumor growth *in vivo*. However, they show a much more significant effect of sorafenib on tumor metastasis than we do. A key difference between these studies is their utilization of partial hepatectomy to remove the primary tumor before initiating sorafenib therapy. These therapies need not be mutually exclusive since they target different pathways. Combination therapy with sorafenib and NanoHHI showed comparable rates of metastasis as Nanno HHI alone (Figure 2B), with, the combination of agents still suppressing Gli1 and Gli2 derived from the tumor cells (Figure 3D). This is not entirely surprising since it is likely multiple pathways contribute to HCC metastasis. Together this suggests Hh activity could account for

a bad prognosis and increased tumor dissemination and taken with our *in vivo* metastasis data, suggests suppressing Gli activity might improve the dismal recurrence rates in HCC.

The possible mechanism of the anti-metastasis efficacy of NanoHHI includes, 1) Inhibition of Hh signaling pathway which has been confirmed as one of the important pathway of cancer initiating/stem cell in our previous studies (unpublished observation and (23)); 2) NanoHHI significantly decreased the population of CD133+ HCC cells, which has been considered as an HCC cancer initiating/stem cells and the source of metastasis and recurrence of HCC. A recent study highlighted the link between Hh activity and CD133 and found well differentiated tumors harbored a CD133 expressing subpopulation that was more tumorgenic requiring less CD133+ cells to initate HCC when injected in the kidney capsule(19). This population of HCC cells provides a reservoir of cells that can self-renew, undergo asymmetric division and might be partially responsible for recurrence after ablative surgery. Furthermore the CD133+ population of cells has also been linked to vascular invasion, resistance to chemoradiotherapy (40, 50).

Supplementary Material

Refer to Web version on PubMed Central for supplementary material.

Acknowledgments

Grant support: This study was combined supported by grants from National Natural Science Foundation of China (No.81030038, 81071661, 30873039); Shanghai Rising-Star Follow-up Program Funds (No. 10QH1400500); National Key Sci-Tech Special Project of Infectious Diseases (No.2008ZX10002-022); National Institute of Health R01DK080736 (R.A.A.); R01DK081417 (R.A.A.); Michael Rolfe Foundation for Pancreatic Cancer Research (A.M. & R.A.A.); U54CA151838 (A.M.), and the Flight Attendants Medical Research Institute (A.M.).

Abbreviations

Hh	Hedgehog signaling
NH	NanoHHI
SO	sorafenib
HCC	hepatocellular carcinoma
Q-RT-PCR	quantitative reverse transcriptase polymerase chain reaction
GAPDH	glyceraldehyde-3-phosphate dehydrogenase
PBS	phosphate-buffered saline
TNM	tumor-node-metastasis
AFP	alpha-fetoprotein
FBS	fetal bovine serum
TMAs	tissue microarrays
OS	overall survival
RFS	relapse free survival
TTR	Time to Recurrence
HBsAg	hepatitis B surface antigen
GGT	gamma-glutamyl transpeptidase

ALT	alanine aminotransferase
BCLC	Barcelona Clinic Liver Cancer
Ptch1	patched homolog 1 protein

Bibliography

1. Llovet JM, Burroughs A, Bruix J. Hepatocellular carcinoma. Lancet. 2003; 362:1907–17. [PubMed: 14667750]
2. Seeff LB. Introduction: The burden of hepatocellular carcinoma. Gastroenterology. 2004; 127:S1–4. [PubMed: 15508071]
3. Lau WY, Lai EC. Hepatocellular carcinoma: current management and recent advances. Hepatobiliary Pancreat Dis Int. 2008; 7:237–57. [PubMed: 18522878]
4. Pawlik TM. Debate: Resection for early hepatocellular carcinoma. J Gastrointest Surg. 2009; 13:1026–8. [PubMed: 19104903]
5. Llovet JM, Ricci S, Mazzaferro V, Hilgard P, Gane E, Blanc JF, et al. Sorafenib in advanced hepatocellular carcinoma. N Engl J Med. 2008; 359:378–90. [PubMed: 18650514]
6. Yau T, Chan P, Ng KK, Chok SH, Cheung TT, Fan ST, et al. Phase 2 open-label study of single-agent sorafenib in treating advanced hepatocellular carcinoma in a hepatitis B-endemic Asian population: presence of lung metastasis predicts poor response. Cancer. 2009; 115:428–36. [PubMed: 19107763]
7. Beachy PA, Karhadkar SS, Berman DM. Tissue repair and stem cell renewal in carcinogenesis. Nature. 2004; 432:324–31. [PubMed: 15549094]
8. Omenetti A, Diehl AM. The adventures of sonic hedgehog in development and repair. II. Sonic hedgehog and liver development, inflammation, and cancer. Am J Physiol Gastrointest Liver Physiol. 2008; 294:G595–8. [PubMed: 18218671]
9. Hooper JE, Scott MP. Communicating with Hedgehogs. Nat Rev Mol Cell Biol. 2005; 6:306–17. [PubMed: 15803137]
10. Deutsch G, Jung J, Zheng M, Lora J, Zaret KS. A bipotential precursor population for pancreas and liver within the embryonic endoderm. Development. 2001; 128:871–81. [PubMed: 11222142]
11. Sicklick JK, Li YX, Choi SS, Qi Y, Chen W, Bustamante M, et al. Role for hedgehog signaling in hepatic stellate cell activation and viability. Lab Invest. 2005; 85:1368–80. [PubMed: 16170335]
12. Sicklick JK, Li YX, Melhem A, Schmelzer E, Zdanowicz M, Huang J, et al. Hedgehog signaling maintains resident hepatic progenitors throughout life. Am J Physiol Gastrointest Liver Physiol. 2006; 290:G859–70. [PubMed: 16322088]
13. Ochoa B, Syn WK, Delgado I, Karaca GF, Jung Y, Wang J, et al. Hedgehog signaling is critical for normal liver regeneration after partial hepatectomy in mice. Hepatology. 2010; 51:1712–23. [PubMed: 20432255]
14. Choi SS, Omenetti A, Witek RP, Moylan CA, Syn WK, Jung Y, et al. Hedgehog pathway activation and epithelial-to-mesenchymal transitions during myofibroblastic transformation of rat hepatic cells in culture and cirrhosis. Am J Physiol Gastrointest Liver Physiol. 2009; 297:G1093–106. [PubMed: 19815628]
15. Omenetti A, Yang L, Li YX, McCall SJ, Jung Y, Sicklick JK, et al. Hedgehog-mediated mesenchymal-epithelial interactions modulate hepatic response to bile duct ligation. Lab Invest. 2007; 87:499–514. [PubMed: 17334411]
16. Berman DM, Karhadkar SS, Maitra A, Montes De Oca R, Gerstenblith MR, Briggs K, et al. Widespread requirement for Hedgehog ligand stimulation in growth of digestive tract tumours. Nature. 2003; 425:846–51. [PubMed: 14520411]
17. Pereira Tde A, Witek RP, Syn WK, Choi SS, Bradrick S, Karaca GF, et al. Viral factors induce Hedgehog pathway activation in humans with viral hepatitis, cirrhosis, and hepatocellular carcinoma. Lab Invest. 2010; 90:1690–703. [PubMed: 20697376]

18. Jung Y, McCall SJ, Li YX, Diehl AM. Bile ductules and stromal cells express hedgehog ligands and/or hedgehog target genes in primary biliary cirrhosis. Hepatology. 2007; 45:1091–6. [PubMed: 17464985]
19. Chen X, Lingala S, Khoobyari S, Nolta J, Zern MA, Wu J. Epithelial Mesenchymal Transition and Hedgehog Signaling Activation are Associated with Chemoresistance and Invasion of Hepatoma Subpopulations. J Hepatol. 2011
20. Chen XL, Cao LQ, She MR, Wang Q, Huang XH, Fu XH. Gli-1 siRNA induced apoptosis in Huh7 cells. World J Gastroenterol. 2008; 14:582–9. [PubMed: 18203291]
21. Chen XL, Cheng QY, She MR, Wang Q, Huang XH, Cao LQ, et al. Expression of sonic hedgehog signaling components in hepatocellular carcinoma and cyclopamine-induced apoptosis through Bcl-2 downregulation in vitro. Arch Med Res. 2010; 41:315–23. [PubMed: 20851287]
22. Chen YJ, Lin CP, Hsu ML, Shieh HR, Chao NK, Chao KS. Sonic Hedgehog Signaling Protects Human Hepatocellular Carcinoma Cells Against Ionizing Radiation in an Autocrine Manner. Int J Radiat Oncol Biol Phys. 2011
23. Cheng WT, Xu K, Tian DY, Zhang ZG, Liu LJ, Chen Y. Role of Hedgehog signaling pathway in proliferation and invasiveness of hepatocellular carcinoma cells. Int J Oncol. 2009; 34:829–36. [PubMed: 19212688]
24. Huang S, He J, Zhang X, Bian Y, Yang L, Xie G, et al. Activation of the hedgehog pathway in human hepatocellular carcinomas. Carcinogenesis. 2006; 27:1334–40. [PubMed: 16501253]
25. Patil MA, Zhang J, Ho C, Cheung ST, Fan ST, Chen X. Hedgehog signaling in human hepatocellular carcinoma. Cancer Biol Ther. 2006; 5:111–7. [PubMed: 16397407]
26. Sicklick JK, Li YX, Jayaraman A, Kannangai R, Qi Y, Vivekanandan P, et al. Dysregulation of the Hedgehog pathway in human hepatocarcinogenesis. Carcinogenesis. 2006; 27:748–57. [PubMed: 16339184]
27. Bisht S, Brossart P, Maitra A, Feldmann G. Agents targeting the Hedgehog pathway for pancreatic cancer treatment. Curr Opin Investig Drugs. 11:1387–98.
28. Buonamici S, Williams J, Morrissey M, Wang A, Guo R, Vattay A, et al. Interfering with resistance to smoothened antagonists by inhibition of the PI3K pathway in medulloblastoma. Sci Transl Med. 2:51ra70.
29. Dijkgraaf GJ, Alicke B, Weinmann L, Januario T, West K, Modrusan Z, et al. Small molecule inhibition of GDC-0449 refractory smoothened mutants and downstream mechanisms of drug resistance. Cancer research. 71:435–44. [PubMed: 21123452]
30. Yauch RL, Dijkgraaf GJ, Alicke B, Januario T, Ahn CP, Holcomb T, et al. Smoothened Mutation Confers Resistance to a Hedgehog Pathway Inhibitor in Medulloblastoma. Science. 2009
31. Hoshida Y, Toffanin S, Lachenmayer A, Villanueva A, Minguez B, Llovet JM. Molecular classification and novel targets in hepatocellular carcinoma: recent advancements. Semin Liver Dis. 2010; 30:35–51. [PubMed: 20175032]
32. Hyman JM, Firestone AJ, Heine VM, Zhao Y, Ocasio CA, Han K, et al. Small-molecule inhibitors reveal multiple strategies for Hedgehog pathway blockade. Proc Natl Acad Sci U S A. 2009; 106:14132–7. [PubMed: 19666565]
33. Chenna V, Hu C, Pramanik D, Aftab BT, Karikari C, Campbell NR, et al. A Polymeric Nanoparticle Encapsulated Small Molecule Inhibitor of Hedgehog Signaling (NanoHHI) Bypasses Secondary Mutational Resistance to Smoothened Antagonists. Molecular Cancer Therapeutics. 2011 In press.
34. Ishak, KG.; Anthony, PP.; Sobin, LH. Nonepithelial tumors. In: Ishak, KG., editor. Histological typing of tumors of the liver. World Health Organization International Classification of tumors. 2. Berlin: Springer; 1994. p. 22-27.
35. Poon RT, Ng IO, Lau C, Yu WC, Yang ZF, Fan ST, et al. Tumor microvessel density as a predictor of recurrence after resection of hepatocellular carcinoma: a prospective study. J Clin Oncol. 2002; 20:1775–85. [PubMed: 11919234]
36. Wittekind C. Pitfalls in the classification of liver tumors. Pathologe. 2006; 27:289–93. [PubMed: 16736177]

37. Gao Q, Qiu SJ, Fan J, Zhou J, Wang XY, Xiao YS, et al. Intratumoral balance of regulatory and cytotoxic T cells is associated with prognosis of hepatocellular carcinoma after resection. J Clin Oncol. 2007; 25:2586–93. [PubMed: 17577038]
38. Cai XY, Gao Q, Qiu SJ, Ye SL, Wu ZQ, Fan J, et al. Dendritic cell infiltration and prognosis of human hepatocellular carcinoma. J Cancer Res Clin Oncol. 2006; 132:293–301. [PubMed: 16421755]
39. Fu X, Wang Q, Chen X, Huang X, Cao L, Tan H, et al. Expression patterns and polymorphisms of PTCH in Chinese hepatocellular carcinoma patients. Exp Mol Pathol. 2008; 84:195–9. [PubMed: 18538319]
40. Lingala S, Cui YY, Chen X, Ruebner BH, Qian XF, Zern MA, et al. Immunohistochemical staining of cancer stem cell markers in hepatocellular carcinoma. Exp Mol Pathol. 2010; 89:27–35. [PubMed: 20511115]
41. Oliva J, French BA, Qing X, French SW. The identification of stem cells in human liver diseases and hepatocellular carcinoma. Exp Mol Pathol. 2010; 88:331–40. [PubMed: 20080086]
42. Vroling L, Lind JS, de Haas RR, Verheul HM, van Hinsbergh VW, Broxterman HJ, et al. CD133+ circulating haematopoietic progenitor cells predict for response to sorafenib plus erlotinib in non-small cell lung cancer patients. Br J Cancer. 2010; 102:268–75. [PubMed: 20010948]
43. Imamura H, Matsuyama Y, Tanaka E, Ohkubo T, Hasegawa K, Miyagawa S, et al. Risk factors contributing to early and late phase intrahepatic recurrence of hepatocellular carcinoma after hepatectomy. J Hepatol. 2003; 38:200–7. [PubMed: 12547409]
44. Nolan-Stevaux O, Lau J, Truitt ML, Chu GC, Hebrok M, Fernandez-Zapico ME, et al. GLI1 is regulated through Smoothened-independent mechanisms in neoplastic pancreatic ducts and mediates PDAC cell survival and transformation. Genes Dev. 2009; 23:24–36. [PubMed: 19136624]
45. Coulouarn C, Factor VM, Thorgeirsson SS. Transforming growth factor-beta gene expression signature in mouse hepatocytes predicts clinical outcome in human cancer. Hepatology. 2008; 47:2059–67. [PubMed: 18506891]
46. Buonamici S, Williams J, Morrissey M, Wang A, Guo R, Vattay A, et al. Interfering with resistance to smoothened antagonists by inhibition of the PI3K pathway in medulloblastoma. Sci Transl Med. 2010; 2:51ra70.
47. Dijkgraaf GJ, Alicke B, Weinmann L, Januario T, West K, Modrusan Z, et al. Small molecule inhibition of GDC-0449 refractory smoothened mutants and downstream mechanisms of drug resistance. Cancer Res. 2011; 71:435–44. [PubMed: 21123452]
48. Yauch RL, Dijkgraaf GJ, Alicke B, Januario T, Ahn CP, Holcomb T, et al. Smoothened mutation confers resistance to a Hedgehog pathway inhibitor in medulloblastoma. Science. 2009; 326:572–4. [PubMed: 19726788]
49. Feng YX, Wang T, Deng YZ, Yang P, Li JJ, Guan DX, et al. Sorafenib suppresses postsurgical recurrence and metastasis of hepatocellular carcinoma in an orthotopic mouse model. Hepatology. 2011; 53:483–92. [PubMed: 21274870]
50. Ma S, Chan KW, Hu L, Lee TK, Wo JY, Ng IO, et al. Identification and characterization of tumorigenic liver cancer stem/progenitor cells. Gastroenterology. 2007; 132:2542–56. [PubMed: 17570225]

Translational Relevance

The Hedgehog (Hh) pathway has been implicated in tumor initiation and metastases in hepatocellular carcinomas (HCCs), and aberrant Hh activation predicts an adverse clinical outcome in patients undergoing curative HCC resection. Current small molecule antagonists of Hh signaling bind to the Smoothened (Smo) receptor. However, secondary mutations of *Smo* and non-canonical activation of the Hh transcription factor Gli are emerging resistance mechanisms used by cancer cells to subvert the effectiveness of Smo antagonists. We have generated a polymeric nanoparticle encapsulated formulation of a novel Gli inhibitor, HPI-1 (“NanoHHI”), which overcomes the systemic bioavailability pitfalls of the parental compound, and blocks Hh signaling directly at the level of Gli function. *In vivo*, NanoHHI potently suppresses the development of HCC metastases in a lethal orthotopic model. Our findings have significant translational relevance in that recurrent metastatic disease represents the single most important basis for mortality following apparently curative HCC resection.

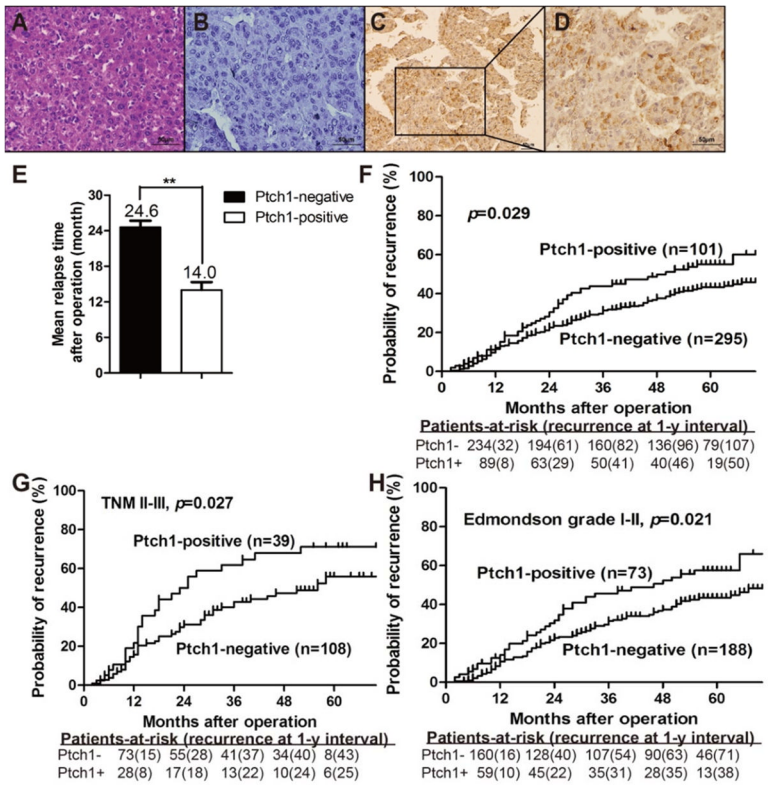

Figure 1. Ptch1 expression in HCC patients

Representative images from TMAs containing 396 patients with HCC. (**A**) H&E and immunohistochemical staining of HCC with (**B**) control IgG and (**C & D**) anti-Ptch1 antibody. (**E**) Mean relapse time for each patient was calculated and compared between HCC's that do and do not express Ptch1. (**F**) Kaplan-Meier analysis showed that high expressing Ptch1 HCCs correlate with a significantly higher rate of tumor recurrence. These trends are most marked in patients with (**G**) advanced stage (TNM II-III) cancers and (**H**) well differentiated (Edmondson grade I-II) histologic grade (D) ** $p < 0.05$.

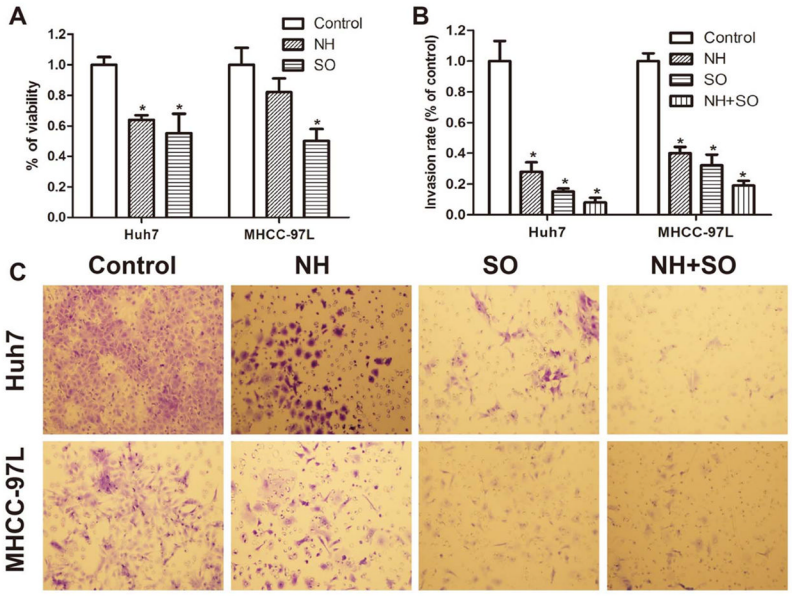

Figure 2. NanoHHI inhibits HCC growth and invasion in vitro

(**A**) Huh7 and MHCC-97L cell lines were treated with NH (NanoHHI 40μm), SO (Sorafenib, 10μm) for 48 hours and viability was determined with MTT assay. (**B**) Huh7 and MHCC-97L cells were seeded onto a Matrigel-coated filter containing NH (40μm), SO (10μm) and NH (40μm)+SO (10μm) for the cell invasion assay and incubated for 8 hours. The cells that actively migrated to the lower surface of the filters were stained (**C**) and quantified and reported as percentage of control.

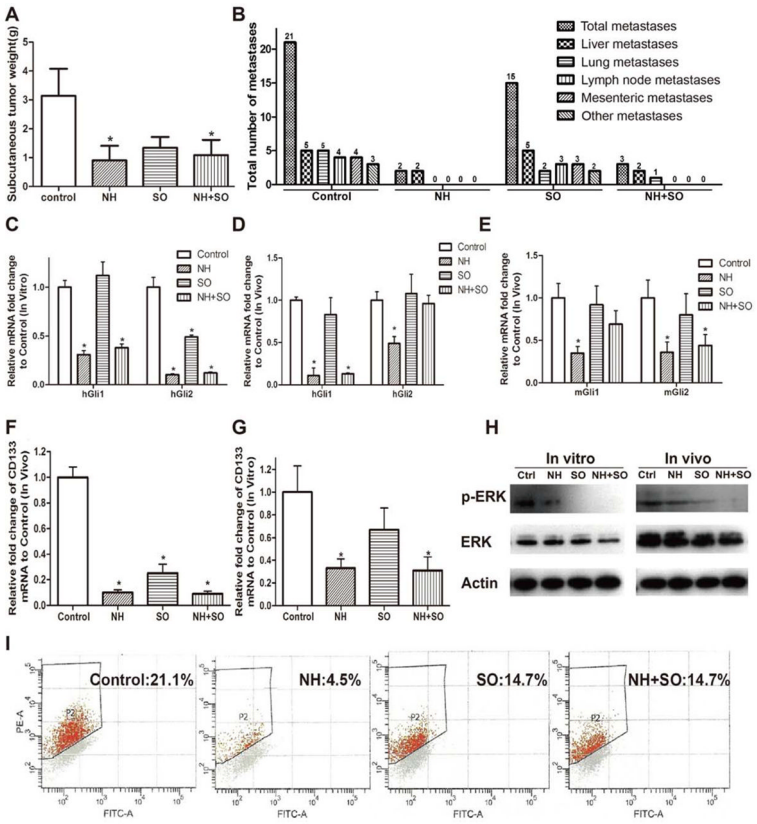

Figure 3. NanoHHI inhibits HCC growth, Gli-1 and Gli-2 expressions, potently suppresses metastasis and decreases CD 133 expression

(A) After 28 days of NH (35mg/kg, i.p, twice a day) and/or SO (20mg/kg, orally gavage, twice a day) treatments, the weight of subcutaneous tumors (Huh7) in nude mice were significantly decreased in the treatment NH and combined NH+SO groups compared with those in control group. **(B)** An 8 mm^3 Huh7 subcutaneous tumor fragment was implanted into each mouse liver and after 7 days mice were randomized to one of four experimental groups. After 28 days of NH (35mg/kg, i.p, twice a day) and/or SO (20mg/kg, orally gavage, twice a day) treatments, metastatic implants were counted in the peritoneum, liver, thorax and lungs by gross and histologic examination. Huh7 Multiple tumor metastases were found in all the mice of control group while NH significantly inhibited tumor metastasis *in vivo*. **(C)** Huh7 cells were untreated (Control) or treated with NH (NanoHHI 40μm), SO (Sorafenib 10μm) and NH (40μm) + SO (10μm) and human Gli-1 and Gli-2 mRNA expressions were determined by Q-RT-PCR after 48 h. (*p<0.05). **(D)** Human Gli-1 and Gli-2 or **(E)** murine Gli-1 and Gli-2 mRNA expressions in orthotopic tumors after 28 days of NH and/or SO treatments *in vivo* was determined with Q-RT-PCR. Expression levels in the treatment groups are expressed relative to untreated (Control) mRNA expression (*p<0.05). **(F)** CD133 mRNA expression in Huh7 orthotopic tumors was determined by Q-RT-PCR in the indicated treatment groups. Untreated (Control), NH (35mg/kg, i.p, twice a day), SO (20mg/kg, orally gavage, twice a day) and NH+SO (*p<0.05). **(G)** Huh7 cells were untreated (Control) or treated with NH (NanoHHI 40μm), SO (Sorafenib 10μm) and NH (40μm) + SO (10μm) and CD133 mRNA expression was determined by Q-RT-PCR (*p<0.01). Data expressed relative to the control treatment where expression was set to 1.0. **(H)** Erk and p-ERK expressions were determined with Western blot after treatment NH and/or SO in vitro and in vivo. **(I)** Flow cytometry analysis showed that NH significantly decreased the population of CD133 positive cells *in vitro* (*p<0.01). All *in vitro* assays were

performed in triplicate, and the mean ± standard deviations are presented. (*$p<0.05$), all compared with control.

Table 1

Univariate analyses of factors associated with survival and recurrence (n=396)

	OS		RFS	
Variables	**Hazard ratio (95% CI)**	**P value**	**Hazard ratio (95% CI)**	**P value**
Sex (male *vs.* female)	1.12(0.72–1.74)	0.631	0.98(0.62–1.55)	0.92
Age, years (>50 *vs.* ≤50)	0.86(0.65–1.14)	0.293	1.07(0.78–1.45)	0.682
HBsAg (positive *vs.* negative)	1.73(1.14–2.64)	0.01	1.08(0.72–1.60)	0.722
HCV (positive *vs.* negative)	0.90(0.37–2.20)	0.822	1.13(0.46–2.76)	0.787
Child-Pugh score (B+C *vs.* A)	1.31(1.02–1.68)	0.033	0.89(0.67–1.18)	0.425
Liver cirrhosis (yes *vs.* no)	0.88(0.63–1.23)	0.448	1.07(0.75–1.51)	0.715
GGT (U/l) (>54 *vs.* ≤54)	1.62(1.20–2.18)	0.001	1.33(0.97–1.82)	0.078
ALT (U/l) (>75 *vs.* ≤75)	0.98(0.60–1.62)	0.944	0.74(0.41–1.34)	0.318
AFP(ng/ml) (>20 *vs.* ≤20)	1.82(1.32–2.50)	0	1.26(0.91–1.75)	0.158
Tumor differentiation (III–IV *vs.* I–II)	1.14(0.85–1.53)	0.376	0.88(0.63–1.23)	0.441
Tumor encapsulation (none *vs.* complete)	0.59(0.45–0.78)	0	0.88(0.65–1.21)	0.441
Tumor size (cm) (>5 *vs.* ≤5)	1.85(1.30–2.65)	0.001	0.88(0.59–1.31)	0.523
Tumor number (multiple *vs.* single)	2.30(1.68–3.15)	0	2.10(1.47–3.00)	0
Vascular invasion (yes *vs.* no)	1.97(1.45–2.67)	0	1.51(1.06–2.14)	0.023
TNM stage (II+III *vs.* I)	2.34(1.76–3.11)	0	1.82(1.33–2.50)	0
BCLC stage (B+C *vs.* 0+A)	1.83(1.36–2.47)	0	1.25(0.91–1.70)	0.166
Ptch1 (positive *vs.* negative)	1.06(0.77–1.46)	0.716	1.48(1.07–2.06)	0.019

Abbreviations: 95%CI, 95% confidence interval; RFS, Relapse-free survival; OS, overall survival. AFP, alpha-fetoprotein; GGT, gamma-glutamyl transpeptidase; ALT, alanine aminotransferase; TACE, transcatheter arterial chemoembolization; TNM, tumor-node-metastasis; BCLC, Barcelona Clinic Liver Cancer; Ptch1, protein patched homolog 1.

Univariate analysis, Cox proportional hazards regression model.

Table 2

Multivariate analyses of factors associated with OS and RFS (n=396)

	OS		RFS	
Variables	**Hazard ratio (95% CI)**	**P value**	**Hazard ratio (95% CI)**	**P value**
HBsAg (positive *vs.* negative)	1.51(0.98–2.33)	0.063	n.a.	
Child-Pugh score (B+C *vs.* A)	1.17(0.91–1.51)	0.218	n.a.	
GGT (U/l) (>54 *vs.* ≤54)	1.35(0.99–1.83)	0.059	n.a.	
AFP(ng/ml) (>20 *vs.* ≤20)	1.49(1.08–2.07)	0.015	n.a.	
Tumor encapsulation (none *vs.* complete)	0.78(0.58–1.05)	0.097	n.a.	
Tumor size (cm) (>5 *vs.* ≤5)	2.08(1.21–3.55)	0.008	n.a.	
Tumor number (multiple *vs.* single)	1.40(0.81–2.40)	0.229	2.05(1.42–2.97)	0
Vascular invasion (yes *vs.* no)	1.20(0.69–2.08)	0.514	1.00(0.72–1.39)	0.994
TNM stage (II+III *vs.* I)	1.76(0.87–3.56)	0.117	1.39(0.96–2.00)	0.078
BCLC stage (B+C *vs.* 0+A)	0.64(0.37–1.10)	0.103	n.a.	
Ptch1 (positive *vs.* negative)	n.a.		1.53(1.09–2.14)	0.013

Abbreviations: OS, overall survival; RFS, relapse-free survival; 95%CI, 95% confidence interval; GGT, gamma-glutamyl transpeptidase; BCLC, Barcelona Clinic Liver Cancer; Ptch1, protein patched were adopted for their prognostic significance by univariate analyses.

Table 3

Univariate analyses of factors associated with survival and recurrence (n=396)

	OS		TTR	
Variables	**Hazard ratio (95% CI)**	**P value**	**Hazard ratio (95% CI)**	**P value**
Sex (male *vs.* female)	1.12(0.72–1.74)	0.631	0.98(0.62–1.55)	0.92
Age, years (>50 *vs.* ≤50)	0.86(0.65–1.14)	0.293	1.07(0.78–1.45)	0.682
HBsAg (positive *vs.* negative)	1.73(1.14–2.64)	0.01	1.08(0.72–1.60)	0.722
HCV (positive *vs.* negative)	0.90(0.37–2.20)	0.822	1.13(0.46–2.76)	0.787
Child-Pugh score (B *vs.* A)	1.31(1.02–1.68)	0.033	0.89(0.67–1.18)	0.425
Liver cirrhosis (yes *vs.* no)	0.88(0.63–1.23)	0.448	1.07(0.75–1.51)	0.715
GGT (U/l) (>54 *vs.* ≤54)	1.62(1.20–2.18)	0.001	1.33(0.97–1.82)	0.078
ALT (U/l) (>75 *vs.* ≤75)	0.98(0.60–1.62)	0.944	0.74(0.41–1.34)	0.318
AFP(ng/ml) (>20 *vs.* ≤20)	1.82(1.32–2.50)	<0.001	1.26(0.91–1.75)	0.158
Tumor differentiation (III–IV *vs.* I–II)	1.14(0.85–1.53)	0.376	0.88(0.63–1.23)	0.441
Tumor encapsulation (none *vs.* complete)	0.59(0.45–0.78)	<0.001	0.88(0.65–1.21)	0.441
Tumor size (cm) (>5 *vs.* ≤5)	1.85(1.30–2.65)	0.001	0.88(0.59–1.31)	0.523
Tumor number (multiple *vs.* single)	2.30(1.68–3.15)	<0.001	2.10(1.47–3.00)	<0.001
Vascular invasion (yes *vs.* no)	1.97(1.45–2.67)	<0.001	1.51(1.06–2.14)	0.023
TNM stage (II+III *vs.* I)	2.34(1.76–3.11)	<0.001	1.82(1.33–2.50)	<0.001
BCLC stage (B+C *vs.* 0+A)	1.83(1.36–2.47)	<0.001	1.25(0.91–1.70)	0.166
Ptch1 (positive *vs.* negative)	1.06(0.77–1.46)	0.716	1.48(1.07–2.06)	0.019

Abbreviations: 95%CI, 95% confidence interval; RFS, Relapse-free survival; OS, overall survival. AFP, alpha-fetoprotein; GGT, gamma-glutamyl transpeptidase; ALT, alanine aminotransferase; TACE, transcatheter arterial chemoembolization; TNM, tumor-node-metastasis; BCLC, Barcelona Clinic Liver Cancer; Ptch1, protein patched homolog 1.

Univariate analysis, Cox proportional hazards regression model.

Table 4

Multivariate analyses of factors associated with OS and TTR (n=396)

	OS		TTR	
Variables	**Hazard ratio (95% CI)**	**P value**	**Hazard ratio (95% CI)**	**P value**
HBsAg (positive *vs.* negative)	1.51(0.98–2.33)	0.063	n.a.	
Child-Pugh score (B *vs.* A)	1.17(0.91–1.51)	0.218	n.a.	
GGT (U/l) (>54 *vs.* ≤54)	1.35(0.99–1.83)	0.059	n.a.	
AFP(ng/ml) (>20 *vs.* ≤20)	1.49(1.08–2.07)	0.015	n.a.	
Tumor encapsulation (none *vs.* complete)	0.78(0.58–1.05)	0.097	n.a.	
Tumor size (cm) (>5 *vs.* ≤5)	2.08(1.21–3.55)	0.008	n.a.	
Tumor number (multiple *vs.* single)	1.40(0.81–2.40)	0.229	2.05(1.42–2.97)	<0.001
Vascular invasion (yes *vs.* no)	1.20(0.69–2.08)	0.514	1.00(0.72–1.39)	0.994
TNM stage (II+III *vs.* I)	1.76(0.87–3.56)	0.117	1.39(0.96–2.00)	0.078
BCLC stage (B+C *vs.* 0+A)	0.64(0.37–1.10)	0.103	n.a.	
Ptch1 (positive *vs.* negative)	n.a.		1.53(1.09–2.14)	0.013

Abbreviations: OS, overall survival; RFS, relapse-free survival; 95%CI, 95% confidence interval; GGT, gamma-glutamyl transpeptidase; BCLC, Barcelona Clinic Liver Cancer; Ptch1, protein patched were adopted for their prognostic significance by univariate analyses.